



Published in final edited form as:

Cancer Res. 2007 March 1; 67(5): 2187–2196. doi:10.1158/0008-5472.CAN-06-3281.

Blockade of Hedgehog Signaling Inhibits Pancreatic Cancer Invasion and Metastases: A New Paradigm for Combination Therapy in Solid Cancers

Georg Feldmann^{1,5}, Surajit Dhara^{1,5}, Volker Fendrich², Djahida Bedja³, Robert Beaty^{1,5}, Michael Mullendore^{1,5}, Collins Karikari^{1,5}, Hector Alvarez^{1,5}, Christine Iacobuzio-Donahue^{1,5}, Antonio Jimeno⁴, Kathleen L. Gabrielson³, William Matsui⁴, and Anirban Maitra^{1,4,5}

¹ Department of Pathology, Johns Hopkins University School of Medicine, Baltimore, Maryland ² Department of Surgery, Johns Hopkins University School of Medicine, Baltimore, Maryland ³ Department of Comparative Medicine, Johns Hopkins University School of Medicine, Baltimore, Maryland ⁴ Department of Oncology, Johns Hopkins University School of Medicine, Baltimore, Maryland ⁵ The Sol Goldman Pancreatic Cancer Research Center, Johns Hopkins University School of Medicine, Baltimore, Maryland

Abstract

In the context of pancreatic cancer, metastasis remains the most critical determinant of resectability, and hence survival. The objective of this study was to determine whether Hedgehog (Hh) signaling plays a role in pancreatic cancer invasion and metastasis because this is likely to have profound clinical implications. In pancreatic cancer cell lines, Hh inhibition with cyclopamine resulted in down-regulation of *snail* and up-regulation of *E-cadherin*, consistent with inhibition of epithelial-to-mesenchymal transition, and was mirrored by a striking reduction of *in vitro* invasive capacity ($P < 0.0001$). Conversely, *Gli1* overexpression in immortalized human pancreatic ductal epithelial cells led to a markedly invasive phenotype ($P < 0.0001$) and near total down-regulation of *E-cadherin*. In an orthotopic xenograft model, cyclopamine profoundly inhibited metastatic spread; only one of seven cyclopamine-treated mice developed pulmonary micrometastases versus seven of seven mice with multiple macrometastases in control animals. Combination of gemcitabine and cyclopamine completely abrogated metastases while also significantly reducing the size of “primary” tumors. *Gli1* levels were up-regulated in tissue samples of metastatic human pancreatic cancer samples compared with matched primary tumors. Aldehyde dehydrogenase (ALDH) overexpression is characteristic for both hematopoietic progenitors and leukemic stem cells; cyclopamine preferentially reduced “ALDH-high” cells by ~3-fold ($P = 0.048$). We confirm pharmacologic Hh pathway inhibition as a valid therapeutic strategy for pancreatic cancer and show for the first time its particular efficacy against metastatic spread. By targeting specific cellular subpopulations likely involved in tumor initiation at metastatic sites, Hh inhibitors may provide a new paradigm for therapy of disseminated malignancies, particularly when used in combination with conventional antimetabolites that reduce “bulk” tumor size.

Requests for reprints: Georg Feldmann, Department of Pathology, Johns Hopkins University School of Medicine, CRB2, Room 316, 1550 Orleans Street, Baltimore, MD 21231. Phone: 410-955-3511; Fax: 410-614-0671; gfeldma4@jhmi.edu.
G. Feldmann and S. Dhara contributed equally to this work.

Note: Supplementary data for this article are available at Cancer Research Online (<http://cancerres.aacrjournals.org/>).

Introduction

Pancreatic cancer is among the most devastating of human malignancies. Despite improvements in surgical and chemotherapeutic approaches during the past decades, pancreatic cancer continues to have a dismal prognosis, with an average overall 5-year survival of <5% (1). To date, surgical resection is the only potentially curative therapeutic option; however, due to the lack of early symptoms, the vast majority of patients present with metastatic disease, rendering their malignancy inoperable (2,3). Even if the disease is diagnosed early and surgical resection with curative intention is done, nearly all patients develop local recurrence and/or distant metastases following surgery and eventually succumb to the debilitating effects of metastatic growth (3). Thus, it is likely that even in the setting of apparently localized disease, micrometastases are present in distant organ sites (4). Conventional chemotherapy is rarely curative for metastatic pancreatic cancer. Treatment strategies that specifically target and prevent metastases might therefore have the potential to significantly improve the prognosis of this dismal disease.

Recently, aberrant activation of the Hedgehog (Hh) pathway has been found in the majority of human pancreatic cancers and other gastrointestinal tract malignancies (5,6). Moderate growth inhibition of 50% to 60% *in vivo* was shown in preestablished s.c. pancreatic cancer xenografts in response to Hh inhibition with the small-molecule smoothened antagonist cyclopamine; the effects were more pronounced when cyclopamine therapy was initiated simultaneously with s.c. implantation of cancer cells (5). Unfortunately, neither of these scenarios, particularly the latter, is clinically relevant. In addition to the established criticisms vis-à-vis s.c. xenograft models and the altered pharmacokinetics in this artificial milieu (7,8), pancreatic cancer xenografts rarely metastasize from the s.c. environment. In the context of a nearly universally metastatic disease like pancreatic cancer, this is a major pitfall. Therefore, to more accurately simulate the cognate human disease scenario, we here tested the effects of Hh blockade using a spontaneously metastasizing xenograft model of pancreatic cancer. Our results confirm that the Hh signaling pathway is a valid therapeutic target in human pancreatic cancer, but, unlike conventional chemotherapeutics that target “bulk” tumor mass, our findings suggest that Hh inhibition has preferential effect on cells responsible for invasion and metastatic seeding.

Materials and Methods

Cell culture

Pancreatic cancer cell lines were grown in either RPMI medium (Invitrogen, Carlsbad, CA) containing 10% fetal bovine serum (FBS; Invitrogen) and 1× penicillin-streptomycin (Biofluids, Camarillo, CA) or in DMEM containing 10% FBS, 1× MEM vitamin solution (Sigma-Aldrich, St. Louis, MO), 1× nonessential amino acid solution, 1% sodium pyruvate solution (both from Biofluids), and 1× penicillin-streptomycin. Human pancreatic ductal epithelial (HPDE) cells were grown in Keratinocyte-SFM, supplemented with 0.1 ng/mL epidermal growth factor and 25 µg/mL bovine pituitary extract (Invitrogen). All cell lines were routinely tested for *Mycoplasma* infection using the MycoSensor PCR Assay Kit (Stratagene, La Jolla, CA).

Cell growth assays

3-(4,5-Dimethylthiazol-2-yl)-2,5-diphenyltetrazolium bromide (MTT) assays were done as previously described (9). In brief, 2,000 cells per well were incubated in 100-µL medium containing 0.5% FBS for 96 h with 6 µmol/L cyclopamine, solvent, or medium only. Finally, 20 µL/well of CellTiter96 solution (Promega, Madison, WI) were added for 1 h and

plates were read on a Wallac-1420 plate reader at an absorbance of 490 nm (Perkin-Elmer, Boston, MA). All experiments were set up in quadruplicate to determine means and SDs.

RNA extraction and real-time reverse transcription-PCR

Tissue samples were homogenized with a rotor stator homogenizer (Polytron PT1200C, Kinematica, Newark, NJ). Cells were lysed in the cell culture dish and RNA was extracted using RNeasy Mini kit (Qiagen, Valencia, CA). RNA was reverse transcribed with oligo-dT primers at 42°C for 50 min using the SuperScript First Strand System (Invitrogen). Quantitative PCR for human or mouse *Gli1*, *Gli2*, *Ptch*, *nestin*, *snail*, and *E-cadherin* was done using either Assays-on-Demand (Applied Biosystems, Foster City, CA) or Quantitect SYBR Green PCR kit (Qiagen) on a 7300 Real-time PCR System. Relative fold levels were determined using the $2(-\Delta\Delta Ct)$ method (10), with *PGK1* used as housekeeping control for human transcripts and *GUSB* for murine assays.

Soft agar assays

Soft agar assays were set up in six-well plates, each well containing a bottom layer of 1% agarose (Invitrogen), a middle layer of 0.6% agarose including 10,000 cells, and a top layer of medium only. Mixtures in each well were supplemented with cyclopamine or solvent where applicable, and the plates were incubated for 3 weeks. Next, 1.5 mL of 0.5% Wright's staining solution were added to each well. After incubation at 4°C overnight, colonies were visualized by trans-UV illumination and counted using analysis software QuantityOne (Bio-Rad, Hercules, CA).

Apoptosis assay

To determine induction of apoptosis, the Guava Multicaspase kit (Guava Technologies, Hayward, CA) was used as we have previously described (9). Briefly, in this assay, the gating of cells occurs as follows: live and noncommitted apoptotic cells, SR-VAD-FMK(-), 7-AAD(-); "early" apoptotic cells: SR-VAD-FMK(+), 7-AAD(-); "late" apoptotic cells, SR-VAD-FMK(+), 7-AAD(+); "dead" cells, SR-VAD-FMK(- or dim), 7-AAD(+).

Cell cycle analysis

After drug treatment, cells were fixed in 70% ethanol, stained with propidium iodide, and analyzed on a Guava Personal Cell Analysis system (Guava Technologies) according to the standard protocol provided by the manufacturer. Percentages of cells in G₀-G₁, S, or G₂-M phase were determined using ModFitLT software version 3.0 (Guava Technologies).

Transient overexpression of Gli1 in HPDE cells

HPDE cells (11) were seeded onto six-well plates at 200,000 per well and transfected the following day with 1 µg of pSR-α-GLI per well or empty vector using FuGene6 transfection reagent (Roche, Indianapolis, IN).

Modified Boyden chamber invasion/migration assays

Modified Boyden chamber assays to assess invasion/migration were done as previously described (12). Briefly, 20 µg/well of Matrigel (BD Biosciences, San Jose, CA) were applied to 24-well transwell plates with 8-µm pore size (BD Biosciences) and allowed to solidify overnight. Then, medium was added and 30,000 cells were seeded into each well. Where applicable, cyclopamine (6 µmol/L) or solvent was added. The assays were done using Panc-1, a Hh-independent cell line, and L3.6pl, a Hh-dependent cell line. The E3LZ10.7 line could not be used in this experiment because, despite multiple attempts, neither control nor treated cells were able to cross the Matrigel barrier. Therefore, L3.6pl cells were used, which show nearly equivalent growth inhibition in response to

cyclopamine. As a converse, Hh signaling was aberrantly activated in HPDE cells by transient transfection of the Hh transcription factor *Gli1*. The plates were incubated at 37°C for 96 h, then cells at the bottom were fixed in ethanol and stained. Cells in 10 randomly selected microscopic fields were counted and means and standard deviations were calculated. Transmigrated cells were normalized for viable cell masses as described (13).

Generation of orthotopic pancreatic cancer xenografts and drug treatment

All animal experiments conformed to the guidelines of the Animal Care and Use Committee of Johns Hopkins University and animals were maintained in accordance to guidelines of the American Association of Laboratory Animal Care. E3LZ10.7 cells [5×10^6 in a total volume of 200 μ L of 1/1 (v/v) PBS/Matrigel] were injected s.c. into male CD1 *nu/nu* athymic mice (Charles River, Wilmington, MA). After 2 to 4 weeks, the s.c. tumors were harvested and cut into cubes of ~ 1 mm³. Male CD1 *nu/nu* athymic mice, ages 6 to 8 weeks, were anesthetized using volatile gas anesthesia. The abdomen was opened via a subcostal left incision of ~ 1 cm. After visualization of the spleen and adherent pancreas, a small pocket was prepared inside the pancreas using microscissors (Roboz Surgical Instruments, Gaithersburg, MD), into which one piece of the s.c. tumor was implanted. The incision in the pancreas was closed with a 8-0 nylon monofilament suture, the abdominal wall was sutured with 6-0 nylon monofilament string, and the skin adapted using wound clips.

In case of L3.6pl, 10^6 cells were resuspended in 50 μ L of a 1:1 (v/v) mixture of PBS/Matrigel and directly injected into the murine pancreas. At 21 days postimplantation of the xenograft, the E3LZ10.7 orthotopic tumor volumes were measured by ultrasound (Vevo660, Visual Sonics, Toronto, Canada). The animals bearing E3LZ10.7 orthotopic xenografts were distributed into four groups with similar average tumor volumes, which were then randomized into four arms: (a) vehicle; (b) cyclopamine, 2 daily doses of 25 mg/kg p.o. by oral gavage; (c) gemcitabine, 100 mg/kg i.p. every 4 days; and (d) combination therapy with cyclopamine plus gemcitabine at the above doses. Cyclopamine was dissolved in a sodium citrate/phosphate buffer (pH 3) containing 10% (w/w) 2-hydroxypropyl- β -cyclodextrin (Sigma-Aldrich) at a concentration of 2.5 mg/mL; gemcitabine was dissolved in 0.9% sodium chloride. The medication was given for a total of 30 days starting 21 days after implantation of the primary xenograft. L3.6pl-bearing mice were treated for 15 days with 50 mg/kg/d of cyclopamine s.c. in a triolein-ethanol vehicle (6).

Necropsy and assessment of primary tumor growth and metastasis

After 30 days of drug treatment, the mice were euthanized; spleen, liver, kidneys, intestine, peritoneum, and lungs were inspected for grossly visible metastases and preserved in 10% formalin solution (Sigma-Aldrich) for histology. Samples of the primary tumors were snap-frozen on dry ice for mRNA analysis. In addition to macroscopic inspection, one random histologic section of liver, spleen, kidneys, lungs, and intestine was examined microscopically for the presence or absence of micrometastases in each animal. Regional lymph nodes were harvested and a histologic section examined if lymph node metastases were suspected from macroscopic inspection.

The series of orthotopic L3.6pl xenografts was only evaluated for the presence of liver and peritoneal metastases.

Immunohistochemical analysis of xenografts

Microscopic slides were prepared from formalin-fixed, paraffin-embedded samples of orthotopic tumors, heated to 60°C for 1 h, deparaffinized using xylene, and hydrated by a graded series of ethanol washes. Antigen retrieval was accomplished by microwave heating in 10 mmol/L sodium citrate buffer (pH 6.0) for 10 min. Endogenous peroxidase activity

was quenched by 10-min incubation in 3% H₂O₂ and nonspecific binding was blocked with 10% serum. Sections were then probed with primary goat anti-human antibodies [Shh (R&D Systems, Minneapolis, MN), Ptch, and nestin (Santa Cruz Biotechnology, Santa Cruz, CA)] in PBS containing 1% FBS overnight at 4°C. After washing twice with PBS, secondary antibodies (1:250) were added for 1 h. Slides were again washed twice with PBS, developed with the Vectastain Elite Kit (Vector Labs, Burlingame, CA) and 3,3'-diaminobenzidine, and counterstained with H&E.

Primary and metastatic pancreatic cancer specimens

Matched samples of primary and metastatic pancreatic cancers were obtained from a pancreatic cancer rapid autopsy program, as previously described (13). Briefly, the tissues are obtained from individuals with terminal, disseminated pancreatic cancer who have provided informed consent for postmortem harvesting of tissue. Eight matched pairs were obtained, including liver, omental, lung, and lymph node metastases with the corresponding primary tumors. Following histopathologic confirmation of neoplastic cellularity, RNA was extracted for reverse transcription-PCR (RT-PCR) analysis.

Evaluation of aldehyde dehydrogenase activity

After incubation with cyclopamine (6 µmol/L) or solvent in low-serum conditions for 3 days, cells were stained for aldehyde dehydrogenase (ALDH) using the Aldefluor reagent (Stem Cell Technologies, Vancouver, Canada) according to the manufacturer's instructions and analyzed on a FACSCalibur flow cytometer (Becton Dickinson). ALDH-positive cells were quantified by calculating the percentage of total cells that displayed greater fluorescence compared with a control staining reaction containing the ALDH inhibitor diethylamino-benzaldehyde.

Statistical analysis

Kruskal-Wallis analysis was done using SPSS version 11.0.1 for Microsoft Windows; two-tailed *t* test and Mann-Whitney *U* test were done using GraphPad Prism for Windows version 4.00. *P* < 0.05 was regarded as statistically significant.

Results

***In vitro* studies establish the metastatic pancreatic cancer cell line E3LZ10.7 as Hh dependent**

A wide range of growth inhibition, from 0% to 100%, was observed in a panel of 21 human pancreatic cancer cell lines in response to 6 µmol/L cyclopamine (Fig. 1A); mostly, this data confirmed previous observations from our and other groups about the variability of *in vitro* responses to cyclopamine in pancreatic cancer cell lines (5,6). For further analysis in the *in vitro* and *in vivo* settings, we selected the low-passage pancreatic cancer cell line E3LZ10.7, which was established from a liver metastasis in a patient with terminally disseminated pancreatic cancer (13). This cell line reproducibly grows in the orthotopic milieu *in vivo*, accompanied by onset of spontaneous metastases, thus enabling the preclinical studies discussed below. Growth inhibition *in vitro* in response to cyclopamine was mirrored by significant down-regulation of the Hh target genes *Gli1* and *Ptch* (Fig. 1B and Supplementary Fig. S1A). Moreover, in the E3LZ10.7 cell line, cyclopamine treatment led to significant down-regulation of *Snail* mRNA and concomitant up-regulation in *E-cadherin* transcripts (Fig. 1C), suggesting inhibition of the epithelial-to-mesenchymal transition phenotype as a result of Hh inhibition. However, cyclopamine treatment resulted only in minor morphologic changes *in vitro*, with a higher percentage of cells undergoing apoptosis (Fig. 1D).

Hh-induced growth inhibition in the E3LZ10.7 line was further accompanied by an increase in the cellular apoptotic fraction, demonstrable by a significant increase of cells in early ($12.0 \pm 0.6\%$ versus $8.4 \pm 0.4\%$; $P = 0.0009$) and late ($5.6 \pm 1.0\%$ versus $1.9 \pm 0.1\%$; $P = 0.0032$) apoptotic states, as well as of dead cells ($9.7 \pm 0.4\%$ versus $4.8 \pm 0.8\%$; $P = 0.0008$; Fig. 2A), and a decrease of the “live cell” fraction ($72.7 \pm 0.4\%$ versus $84.9 \pm 0.8\%$; $P < 0.0001$; not shown) as determined by the Guava MultiCaspase assay. Cyclopamine treatment in low-serum conditions caused minor albeit reproducible increases in the fraction of cells in the G₀-G₁ phase of the cell cycle (72.3% versus 67.1%) and decreased the amounts of cells in S phase (16.75% versus 21.37%) or G₂-M phase (10.92% versus 11.53%; Fig. 2B), suggesting that the major contribution of growth inhibition occurs through increased cell death rather than reduced proliferation. We then explored the effects of Hh blockade on *in vitro* tumorigenicity using colony formation in soft agar as a read-out. Although Hh inhibition with cyclopamine did not completely abolish anchorage-independent growth in this cell line, colony formation in soft agar was significantly reduced compared with vehicle-treated cells (72.7 ± 7.1 versus 119.3 ± 9.3 colonies, respectively; $P = 0.002$). In contrast, cyclopamine did not affect anchorage-independent growth of Panc-1 cells (Fig. 2C), which was shown to be Hh independent based on the lack of response in MTT assays (Fig. 1A) and the absence of target gene down-regulation (data not shown).

Hh signaling modulates the invasive phenotype of pancreatic epithelium independent of proliferation

Having established the contribution of Hh signaling to *in vitro* growth, we wanted to further dissect whether this pathway has an effect on the invasive phenotype, a critical measure of cancer dissemination. In modified Boyden chamber assays, Hh-dependent L3.6pl cells treated with cyclopamine showed a >500-fold reduction in the number of transmigrating cells ($P < 0.0001$), and this phenomenon was independent of inhibition of cell growth (Fig. 2D). In contrast, no effects on the invasive properties of the Hh-independent cell line Panc-1 were seen with cyclopamine treatment (Fig. 2D). We then carried out these assays from the reciprocal perspective (i.e., by aberrantly overexpressing the Hh transcription factor *Gli1* in an immortalized, nontransformed HPDE cell line and determining the effects of such ectopic expression on cell growth and invasion). We first determined that parental HPDE cells have minimal endogenous Hh activity as gauged by reporter studies and target gene expression (data not shown). We then confirmed that ectopic Hh activation in HPDE cells results in increased cell growth compared with mock-transfected cells ($P = 0.029$; Fig. 3A); therefore, invasion assays were normalized to the viable cell count to exclude any effects of increased cell number on transmigration. Independent of cell growth, *Gli1* overexpression had profound and significant effects on the invasive properties of HPDE cells at 96 h compared with mock-transfected cells ($P < 0.0001$; Fig. 3B) but did not induce any morphologic changes *in vitro* (not shown).

Cyclopamine abrogates metastases in an orthotopic xenograft model of pancreatic cancer and synergizes with gemcitabine

Surgical orthotopic implantation was well tolerated by athymic mice, and the tumor take rate was 100%. No obvious side effects or behavioral disturbances of either cyclopamine or gemcitabine, alone or in combination, at the given doses were observed during the 30 days of treatment, and there were no differences in body weight between the four respective treatment groups caused by the medication (Fig. 4A). However, one of the seven mice in group D (cyclopamine + gemcitabine) died after 12 days of treatment of unknown reason (necropsy could not be done) and, therefore, only six mice were analyzed in this group. Cyclopamine treatment did not significantly inhibit E3LZ10.7 primary tumor growth as gauged by the orthotopic tumor volumes at the end of treatment, although primary tumors in the cyclopamine group tended to be smaller than those of the control group ($P = 0.097$). In

contrast, gemcitabine inhibited growth of the primary tumors as compared with both mock-treated ($P < 0.001$) and cyclopamine-treated animals ($P = 0.004$). Combination of cyclopamine with gemcitabine treatment had no additional effect on inhibition of primary tumor growth as compared with gemcitabine alone, but significantly reduced tumor growth as compared with cyclopamine only ($P = 0.001$; Fig. 4B).

Whereas cyclopamine therapy had no significant effects on E3LZ10.7 primary tumor growth, the effects on tumor metastases were profound (Table 1). At the end of 30 days of systemic therapy, distant metastases were present in all of the seven (100%) vehicle-treated control animals as seen macroscopically and in histologic sections (Fig. 5A and B); specifically, 6 of 7 had spleen, 4 of 7 liver, 3 of 7 regional lymph node, and 2 animals had peritoneal and kidney metastases, respectively. In contrast, only 1 of 7 (14%) mice exhibited histologically demonstrable micrometastases to the lung in treatment group B (cyclopamine only), whereas metastases were completely absent in animals receiving combination therapy with cyclopamine and gemcitabine (group D). In mice treated with gemcitabine only (group C), there were metastases to the spleen in 3 of 7 and to regional lymph nodes in 1 of 7 cases, but no metastases to other organ sites were found.

Our first experiments using an orthotopic injection technique had also shown inhibition of metastases in xenografts of another pancreatic cancer cell line, L3.6pl (Supplementary Table S1). Whereas liver metastases developed in 9 of 9 (100%) control animals and peritoneal metastases were present in 4 of 9 (44%) control cases, no metastases were found in cyclopamine-treated mice.

There were no obvious morphologic differences in the primary E3LZ10.7 tumors between the controls and cyclopamine-treated xenografts. However, in xenografts that had received gemcitabine, with or without cyclopamine, histologic sections showed prominence of single pleomorphic cancer cells as opposed to confluent sheets of necrotic tumor cells, as well as prominence of residual stromal cells (Fig. 5C). In concert with the lack of histologic distinctions between control and cyclopamine-treated animals, no differences were found in the immunohistochemical expression of the Hh ligand Shh and the Hh receptor Ptch, with abundant expression observed in both arms (data not shown). Nestin immunohistochemistry, which was used to highlight tumor neovasculature of murine origin (14,15), also revealed no significant differences between cyclopamine and control arms (Fig. 5D).

A variety of pharmacodynamic parameters were then examined in the primary xenografts from the four treatment arms. Murine nestin is expressed in the tumor neovasculature of xenografts (14,15), whereas the human nestin assay is expected to detect any nestin expression within the neoplastic cells themselves. Quantitative RT-PCR analysis showed significant down-regulation of murine nestin mRNA in the treatment groups receiving gemcitabine, with or without addition of cyclopamine, compared with the control arm, which is consistent with reduction in tumor neovasculature, whereas no significant differences were noted between control and cyclopamine-only groups. Human nestin levels showed a trend towards decreased expression in both treatment groups that received cyclopamine; however, due to the small sample number and considerable variation between the respective samples, these differences did not reach statistical significance (Fig. 5D). Murine *Ptch* levels, reflecting Hh expression in the stromal components, showed a trend towards decreased expression in the treatment groups; however, because this decrement was also observed in the gemcitabine arm, the mechanism-based significance is uncertain. We saw no significant differences or trends in the expression of human *Ptch* (Fig. 5D); similarly, there were no significant differences or trends in murine or human *Gli1* or *Gli2* mRNA (data not shown). No significant differences in *snail* mRNA levels could be observed, again possibly because the sample numbers studied were too small (Fig. 5D).

Gli1 is overexpressed in human pancreatic cancer metastases

In light of our consistent *in vitro* and *in vivo* experimental observations correlating Hh signaling with the invasive and metastatic capacity of pancreatic cancer cells, we examined eight matched primary and metastasis samples obtained at rapid (“warm”) autopsy from patients with disseminated pancreatic cancer. We found significant overexpression of Gli1 transcripts in 4 of 8 (50%) matched metastatic foci as compared with the primary tumors (Fig. 6A); snail transcripts were overexpressed in 3 of 4 studied cases (data not shown).

Cyclopamine treatment preferentially reduces the ALDH-expressing population in pancreatic cancer cells

Expression of elevated ALDH levels is associated with a stem/progenitor cell phenotype in the hematopoietic system (16–18); moreover, the expression of elevated ALDH within leukemic cells segregates with a subpopulation capable of tumor engraftment on serial transplantation assays (19). The establishment of distant metastases can be considered analogous to “tumor initiation” at a distant site. Given the profound effect of cyclopamine therapy on limiting pancreatic cancer metastases, we wanted to determine whether Hh blockade would result in selective depletion of ALDH-expressing cells. Treatment with 6 $\mu\text{mol/L}$ cyclopamine reproducibly and preferentially reduced the percentage of ALDH-expressing E3LZ10.7 cells by ~3-fold ($P = 0.048$; Fig. 6B), suggesting that blockade of Hh signaling might specifically eliminate the subpopulation of cells with putative tumor-initiating properties.

Interestingly, significant overexpression of Gli mRNA was found in “ALDH-bright” E3LZ10.7 versus unsorted cells by quantitative RT-PCR, whereas Ptch and E-cadherin expression was not significantly different (Fig. 6C).

Discussion

Studies conducted by two groups, including ours, were the first to show that aberrant activation of the Hh pathway occurs in the majority of pancreatic cancers (6). Moreover, this ectopic activation seems to be due to Hh ligand overexpression rather than to activating mutations of genes involved in Hh signaling. This offers a unique opportunity to study pharmacologic Hh pathway inhibition by means of the small-molecule *smoothed* inhibitor cyclopamine as a new therapeutic strategy for pancreatic cancer. Whereas blockade of Hh signaling causes growth inhibition of Hh-dependent pancreatic cancer cell lines *in vitro* and a modest growth inhibition of the resulting s.c. pancreatic cancer xenografts *in vivo* (5,6), the effects on pancreatic cancer metastases remain unexplored. To our knowledge, this is the first report specifically showing the potential for Hh inhibitors as a therapeutic option for limiting pancreatic cancer metastases. Thus, only one lung micrometastasis was observed in one of seven E3LZ10.7-bearing cyclopamine-treated mice, and complete absence of metastases was observed in xenografted mice treated with the combination therapy of cyclopamine and gemcitabine. Most notably, the striking reduction in pancreatic cancer metastases was present despite the apparent lack of significant effect of cyclopamine monotherapy on bulk primary tumor volume.

This abrogation of metastasis was also observed in xenografts derived from another pancreatic cancer cell line, L3.6pl, precluding this being only a special feature of one particular cell line.

For the first time, our study addresses two critical issues pertaining to the role of Hh pathway as a therapeutic target in pancreatic cancer. First, we show the significant correlation between extent of intracellular Hh activation and invasive ability, which is independent of any effects this signaling pathway may have on proliferation. Blockade of

Hh signaling in pancreatic cancer cells significantly inhibits invasion, and, conversely, ectopic Hh activation in immortalized human pancreatic ductal cells renders them profoundly invasive in modified Boyden chamber assays. It has been previously reported that an active Hh pathway induces epithelial-to-mesenchymal transition through *Gli1*-dependent transcriptional down-regulation of the cell adhesion molecule *E-cadherin* (12,20,21), which, in turn, confers a greater invasive ability in cancer cells (20,21). Our data confirm that similar mechanisms are active in the pancreatic epithelium, with profound loss of *E-cadherin* expression in HPDE-*Gli1* cells and the reciprocal up-regulation of *E-cadherin* in E3LZ10.7 cells treated with cyclopamine.

The second issue that we address in this study pertains to minor cellular subpopulations that may be preferentially affected by Hh blockade in pancreatic cancer. Specifically, we show an ~3-fold reduction in the proportion of ALDH-expressing cells by cyclopamine therapy in E3LZ10.7 cells. Our finding of *Gli* overexpression in ALDH-bright cells might suggest that this subpopulation could be particularly Hh dependent and, therefore, preferentially sensitive to Hh inhibition with cyclopamine.

Expression of elevated ALDH levels in human hematopoietic progenitor cells was first reported more than 15 years ago; subsequently, the “ALDH-high” cells were shown to have significantly higher levels of engraftment when transplanted into nonobese diabetic/severe combined immunodeficient mice (17,18,22). More recently, lineage-negative, ALDH-high cells isolated from acute leukemias were shown to have consistent ability to engraft in nonobese diabetic/severe combined immunodeficient mice, which is consistent with this subpopulation being enriched in leukemic stem cells (19). The ~3-fold reduction of cells with elevated ALDH expression in treated E3LZ10.7 cells suggests that cyclopamine might be preferentially targeting the putative tumor-initiating subpopulation in pancreatic cancers, rather than the proliferative fraction comprising the bulk tumor volume.

How do we reconcile these two discrete effects of cyclopamine therapy, i.e., impairment of invasive capacity within the overall population of pancreatic cancer cells and a preferential depletion of a minor subpopulation of ALDH-expressing cells, in the context of observed *in vivo* effects on metastasis inhibition? To address this question, one must consider the process of metastasis as one of tumor initiation occurring at a distant anatomic site. Given the numbers of cells released by a primary tumor into circulation per day (usually in millions) and the relatively few established metastases one encounters, the vast majority of disseminated cancer cells reaching potential metastatic sites are incapable of engraftment, and only a minority of circulating tumor cells retain the potential capacity to result in tumor initiation at secondary foci. Arguably then, a reduction in metastases can be observed with therapies that either limit the overall numbers of disseminated cells in circulation or with therapies that cause selective depletion of tumor-initiating cells even in the absence of discernible effects on cells that comprise the bulk of the tumor. For example, gemcitabine treatment significantly inhibited primary tumor growth in our series and concurrently reduced, but did not completely abrogate, the occurrence of macrometastases in the orthotopic xenograft model, which is consistent with previous reports (23). Conventional antimetabolites such as gemcitabine likely reduce metastasis incidence by a sheer decrement in bulk tumor volume and proportional reduction in numbers of circulating tumor cells. In contrast, cyclopamine has a negative effect on metastatic seeding in pancreatic cancer that dramatically exceeds the observed efficacy on primary tumor volume, suggesting that cyclopamine either (a) inhibits the functional ability of cancer cells to invade (e.g., by down-regulation of epithelial-to-mesenchymal transition) or (b) preferentially targets the minor proportion of cells capable of tumor initiation within the bulk tumor without necessarily reducing overall invasive capacity, or (c) results in a combination of (a) and (b). In contrast to gemcitabine, which unequivocally alters xenograft morphology, we find no significant

histologic differences between control and cyclopamine-treated primary tumors, underscoring what we observe at the macroscopic level. Similarly, we find no differences in stromal neovasculature (as assessed by murine nestin immunohistochemistry and real-time PCR) between control and cyclopamine-treated arms, arguing against the possibility that reduced passive “leakage” of tumor cells into the circulation might account for the reduced frequency of metastases.

It is entirely possible that the lack of tumor growth inhibition in the orthotopic location is merely a pharmacokinetic issue that can be overcome with higher dosing. A previous report by Thayer et al. (5), using s.c. xenograft models and delayed administration of cyclopamine (i.e., onset of cyclopamine treatment after s.c. xenografts became palpable), had shown a modest growth inhibition of 50% to 60% in two pancreatic cancer lines. Notably, even in this study, “concurrent” administration of cyclopamine (i.e., onset of cyclopamine treatment in conjunction with s.c. injection of cells) resulted in a more profound effect on xenograft growth inhibition (~80%), confirming that this class of agents has a greater effect on preventing tumor initiation than on established tumor regression. This finding is entirely compatible with our observed preferential effects on limiting metastases in the orthotopic model. Given a persistent requirement for Hh signaling in maintaining tissue homeostasis, one needs to be cognizant of potential toxicities that might arise from higher cyclopamine dosages in somatic Hh-dependent cell populations. Consistent with previous reports (reviewed in ref. 24), we found no obvious signs of toxicity by Hh inhibition with cyclopamine at the given dose (25 mg/kg p.o. by oral gavage twice daily) in mice during the 30-day treatment period. It is possible that somatic stem cells, much like the bulk tumor cell population, are less Hh dependent than the circulating cancer cells that are destined to engraft at metastatic sites; however, this remains a matter of speculation.

We believe that our results provide a compelling rationale for exploring Hh inhibitors in human pancreatic cancer, particularly from the standpoint of therapy of metastatic disease. Despite small numbers, we show that the Hh transcription factor *Glil* is overexpressed at the mRNA level in four of eight samples from pancreatic cancer metastases as compared with matched primary tumor tissue, underscoring a role for this pathway in mediating disease progression. From an experimental therapeutics perspective, we also present an improvement in cyclopamine formulation that will facilitate its clinical translation. In previous preclinical reports, cyclopamine was usually administered dissolved in a triolein/ethanol or DMSO base, with adverse reactions (ulcerations) commonly seen at the injection site. In this study, we have used an orally bioavailable formulation of cyclopamine dissolved in cyclodextrin, which was administered by oral gavage at a twice-daily dosing schedule. Other orally bioavailable Hh small-molecule inhibitors have also been reported (25) and, together with the current formulation or its analogues, are likely to be used in future clinical trials.

In summary, we show for the first time that cyclopamine has a profound effect in limiting pancreatic cancer metastases *in vivo*. Our results potentially serve as the seedbed for a new paradigm in anticancer therapy, wherein a conventional antimetabolite that reduces bulk tumor volume (e.g., gemcitabine) is combined with a class of metastasis inhibitors like cyclopamine to enhance overall therapeutic efficacy and eventually ameliorate survival.

Supplementary Material

Refer to Web version on PubMed Central for supplementary material.

Acknowledgments

Grant support: NIH grants R01CA113669 and R21DK072532, the Sol Goldman Pancreatic Cancer Research Center, and an AACR-PanCAN award (A. Maitra), and fellowship grant within the Postdoc-Programme of the German Academic Exchange Service (DAAD) (G. Feldmann).

We thank Infinity Pharmaceuticals (Cambridge, MA) for the kind donation of cyclopamine.

References

1. Jemal A, Siegel R, Ward E, et al. Cancer statistics, 2006. *CA Cancer J Clin.* 2006; 56:106–30. [PubMed: 16514137]
2. Warshaw AL, Fernandez-del Castillo C. Pancreatic carcinoma. *N Engl J Med.* 1992; 326:455–65. [PubMed: 1732772]
3. Li D, Xie K, Wolff R, Abbruzzese JL. Pancreatic cancer. *Lancet.* 2004; 363:1049–57. [PubMed: 15051286]
4. Schneider G, Siveke JT, Eckel F, Schmid RM. Pancreatic cancer: basic and clinical aspects. *Gastroenterology.* 2005; 128:1606–25. [PubMed: 15887154]
5. Thayer SP, di Magliano MP, Heiser PW, et al. Hedgehog is an early and late mediator of pancreatic cancer tumorigenesis. *Nature.* 2003; 425:851–6. [PubMed: 14520413]
6. Berman DM, Karhadkar SS, Maitra A, et al. Widespread requirement for Hedgehog ligand stimulation in growth of digestive tract tumours. *Nature.* 2003; 425:846–51. [PubMed: 14520411]
7. Kerbel RS. Human tumor xenografts as predictive preclinical models for anticancer drug activity in humans: better than commonly perceived-but they can be improved. *Cancer Biol Ther.* 2003; 2:S134–9. [PubMed: 14508091]
8. Kelland LR. Of mice and men: values and liabilities of the athymic nude mouse model in anticancer drug development. *Eur J Cancer.* 2004; 40:827–36. [PubMed: 15120038]
9. Sui G, Bonde P, Dhara S, et al. Epidermal growth factor receptor and hedgehog signaling pathways are active in esophageal cancer cells from rat reflux model. *J Surg Res.* 2006; 134:1–9. [PubMed: 16488438]
10. Livak KJ, Schmittgen TD. Analysis of relative gene expression data using real-time quantitative PCR and the $2(-\Delta\Delta C(T))$ method. *Methods.* 2001; 25:402–8. [PubMed: 11846609]
11. Furukawa T, Duguid WP, Rosenberg L, Viallet J, Galloway DA, Tsao MS. Long-term culture and immortalization of epithelial cells from normal adult human pancreatic ducts transfected by the E6E7 gene of human papilloma virus 16. *Am J Pathol.* 1996; 148:1763–70. [PubMed: 8669463]
12. Karhadkar SS, Bova GS, Abdallah N, et al. Hedgehog signalling in prostate regeneration, neoplasia and metastasis. *Nature.* 2004; 431:707–12. [PubMed: 15361885]
13. Embuscado EE, Laheru D, Ricci F, et al. Immortalizing the complexity of cancer metastasis: genetic features of lethal metastatic pancreatic cancer obtained from rapid autopsy. *Cancer Biol Ther.* 2005; 4:548–54. [PubMed: 15846069]
14. Amoh Y, Yang M, Li L, et al. Nestin-linked green fluorescent protein transgenic nude mouse for imaging human tumor angiogenesis. *Cancer Res.* 2005; 65:5352–7. [PubMed: 15958583]
15. Amoh Y, Li L, Tsuji K, et al. Dual-color imaging of nascent blood vessels vascularizing pancreatic cancer in an orthotopic model demonstrates antiangiogenesis efficacy of gemcitabine. *J Surg Res.* 2006; 132:164–9. [PubMed: 16500746]
16. Storms RW, Trujillo AP, Springer JB, et al. Isolation of primitive human hematopoietic progenitors on the basis of aldehyde dehydrogenase activity. *Proc Natl Acad Sci U S A.* 1999; 96:9118–23. [PubMed: 10430905]
17. Storms RW, Green PD, Safford KM, et al. Distinct hematopoietic progenitor compartments are delineated by the expression of aldehyde dehydrogenase and CD34. *Blood.* 2005; 106:95–102. [PubMed: 15790790]
18. Hess DA, Meyerrose TE, Wirthlin L, et al. Functional characterization of highly purified human hematopoietic repopulating cells isolated according to aldehyde dehydrogenase activity. *Blood.* 2004; 104:1648–55. [PubMed: 15178579]

19. Pearce DJ, Taussig D, Simpson C, et al. Characterization of cells with a high aldehyde dehydrogenase activity from cord blood and acute myeloid leukemia samples. *Stem Cells*. 2005; 23:752–60. [PubMed: 15917471]
20. Huber MA, Kraut N, Beug H. Molecular requirements for epithelial-mesenchymal transition during tumor progression. *Curr Opin Cell Biol*. 2005; 17:548–58. [PubMed: 16098727]
21. Zhou BP, Hung MC. Wnt, hedgehog and snail: sister pathways that control by GSK-3 β and β -Trcp in the regulation of metastasis. *Cell Cycle*. 2005; 4:772–6. [PubMed: 15917668]
22. Hess DA, Wirthlin L, Craft TP, et al. Selection based on CD133 and high aldehyde dehydrogenase activity isolates long-term reconstituting human hematopoietic stem cells. *Blood*. 2006; 107:2162–9. [PubMed: 16269619]
23. Bauer TW, Liu W, Fan F, et al. Targeting of urokinase plasminogen activator receptor in human pancreatic carcinoma cells inhibits c-Met- and insulin-like growth factor-I receptor-mediated migration and invasion and orthotopic tumor growth in mice. *Cancer Res*. 2005; 65:7775–81. [PubMed: 16140945]
24. Lees C, Howie S, Sartor RB, Satsangi J. The hedgehog signalling pathway in the gastrointestinal tract: implications for development, homeostasis, and disease. *Gastroenterology*. 2005; 129:1696–710. [PubMed: 16285967]
25. Romer JT, Kimura H, Magdaleno S, et al. Suppression of the Shh pathway using a small molecule inhibitor eliminates medulloblastoma in Ptc1(+/-)p53(-/-) mice. *Cancer Cell*. 2004; 6:229–40. [PubMed: 15380514]

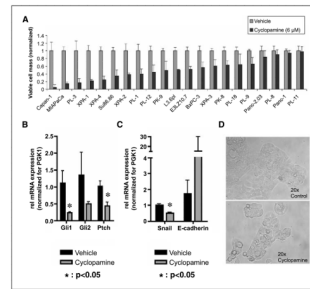


Figure 1.

A, viable cell masses, determined using MTT assays, were reduced by nearly 100% to 0% by Hh inhibition with 6 $\mu\text{mol/L}$ cyclopamine for 4 d as compared with solvent-treated cells *in vitro*. B, on treatment with cyclopamine, RT-PCR revealed down-regulation of the Hh target genes *Gli1* and *Ptc1* on the mRNA level in the pancreatic cancer cell line E3LZ10.7. C, Hh inhibition with cyclopamine led to down-regulation of *Snail* and up-regulation of *E-cadherin* mRNA in E3LZ10.7 *in vitro*. D, microscopic photographs of E3LZ10.7 cells treated with cyclopamine (6 $\mu\text{mol/L}$) or solvent for 4 d.

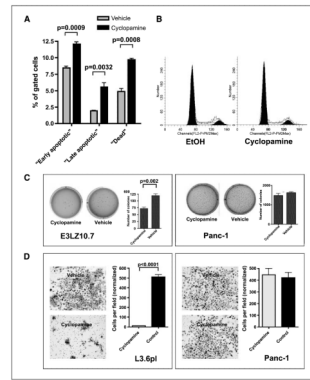


Figure 2.

A, using the Guava Multicaspase assay, an increase of cells undergoing apoptosis was detected on treatment with cycloamine. *B*, cycloamine treatment slightly but reproducibly increased the percentage of cells in G₀-G₁ phase, whereas the fractions of cells in S and G₂-M phases were reduced. Representative of three independent experiments with similar results using the Guava Cell Cycle analysis kit. *C*, anchorage-independent growth in soft agar was reduced in the Hh-sensitive cell line E3LZ10.7 on Hh inhibition with cycloamine, whereas treatment with cycloamine showed no effect on the Hh-resistant cell line Panc-1. *D*, inhibition of invasion/migration of the Hh-dependent metastatic pancreatic cancer cell line L3.6pl *in vitro* by cycloamine treatment. Cycloamine had no effect on Panc-1 cells.

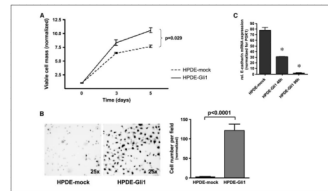


Figure 3.

Transient overexpression of Gli1 led to increased proliferation as determined by MTT assays (A) and invasion/migration (B) *in vitro* in the immortalized normal ductal epithelial cell line HPDE. Transient overexpression of the transcription factor Gli1 led to down-regulation of E-Cadherin in a time-dependent manner as revealed by real-time RT-PCR (C). *, statistically significant differences as compared with control cells.

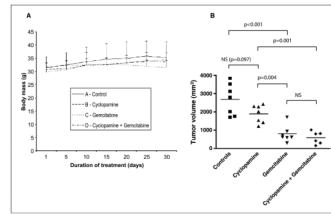


Figure 4.

A, during the 30 d of treatment, there was no difference in body weights between mice treated with vehicle alone, cyclophamide, gemcitabine, or combination therapy with gemcitabine plus cyclophamide. B, tumor sizes of primary xenografted tumors at the end of treatment. Tumors in the cyclophamide group were not significantly smaller than in the control group. Treatment with gemcitabine led to significantly reduced average tumor size as compared with vehicle or cyclophamide. Combination of cyclophamide with gemcitabine was not superior to treatment with gemcitabine alone in controlling primary tumor growth.

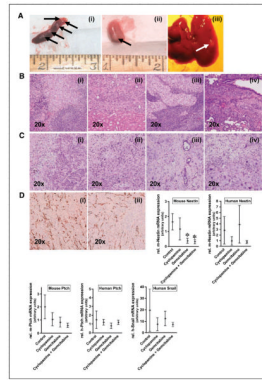


Figure 5.

A, distant metastases of the primary xenograft to spleen (*i*), kidney (*ii*), and liver (*iii*). B, histologic images of spleen (*i*), kidney (*ii*), and lymph node metastases (*iii*). In one animal receiving monotherapy with cyclophosphamide, micrometastases to the lung were detected in a histologic slide (*iv*). C, histologies of xenograft tumors treated with vehicle (*i*), cyclophosphamide (*ii*), gemcitabine (*iii*), or combination of cyclophosphamide plus gemcitabine (*iv*) after 30 d of treatment. D, Hh target gene expression in orthotopic pancreatic cancer xenografts. Immunohistochemistry for nestin in vehicle-treated (*i*) and cyclophosphamide-treated (*ii*) tumor tissues. The diagrams show relative steady-state mRNA expression of murine and human nestin and patched, as well as human snail. *Points*, mean; *bars*, SD. *, statistically significant difference as compared with the control group.

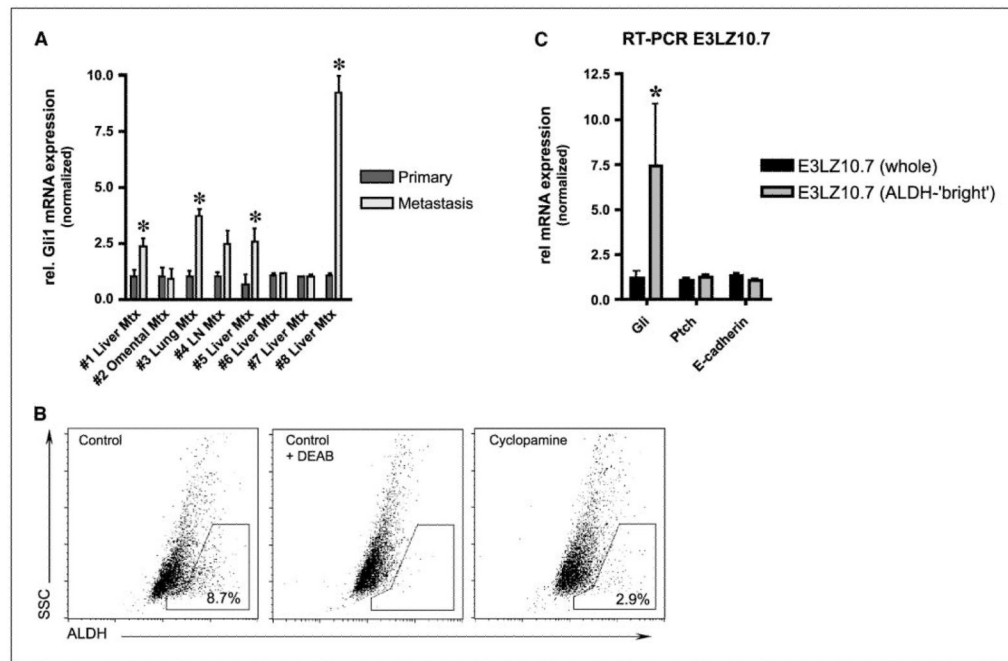


Figure 6.

A, in matched human tissue samples, Gli1 mRNA was found to be up-regulated in metastatic nodules as compared with the primary tumors in four of eight studied cases. *B*, flow cytometry revealed an ~3-fold reduction in ALDH-high cells on treatment with cyclopamine *in vitro* ($P = 0.048$). Representative data of two experiments with similar results. *C*, quantitative real-time RT-PCR analysis revealed overexpression of Gli mRNA in flow-sorted ALDH-bright E3LZ10.7 as compared with unsorted cells. Expression of Ptch and E-cadherin was not markedly changed. *, $P < 0.05$.

Table 1

Numbers of animals with metastases to distant organ sites in the different treatment groups of E3LZ10.7 xenografts

Group	A	B	C	D
Regimen	Vehicle	Cyclopamine	Gemcitabine	Cyclopamine + gemcitabine
No. animals	7	7	7	6
Spleen	6/7 (86%)	0/7 (0%)	3/7 (43%)	0/6 (0%)
Liver	4/7 (57%)	0/7 (0%)	0/7 (0%)	0/6 (0%)
Lymph nodes	3/7 (43%)	0/7 (0%)	1/7 (14%)	0/7 (0%)
Peritoneum	2/7 (29%)	0/7 (0%)	0/7 (0%)	0/6 (0%)
Kidneys	2/7 (29%)	0/7 (0%)	0/7 (0%)	0/6 (0%)
Lungs	0/7 (0%)	1/7 (14%)	0/7 (0%)	0/6 (0%)
Intestine	0/7 (0%)	0/7 (0%)	0/7 (0%)	0/6 (0%)